Bioorganic & Medicinal Chemistry 20 (2012) 3746–3755

Contents lists available at SciVerse ScienceDirect

Bioorganic & Medicinal Chemistry

journal homepage: www.elsevier.com/locate/bmc

Synthesis, biological evaluation and 3D-QSAR studies of novel 4,5-dihydro-1*H*-pyrazole niacinamide derivatives as BRAF inhibitors

Cui-Yun Li [a,†], Qing-Shan Li [a,†], Li Yan [a], Xiao-Guang Sun [a], Ran Wei [a], Hai-Bin Gong [b,*], Hai-Liang Zhu [a,*]

[a] State Key Laboratory of Pharmaceutical Biotechnology, Nanjing University, Nanjing 210093, PR China
[b] Xuzhou Central Hospital, Xuzhou 221009, PR China

ARTICLE INFO

Article history:
Received 10 March 2012
Revised 21 April 2012
Accepted 23 April 2012
Available online 28 April 2012

Keywords:
Synthesis
Antitumor activity
4,5-Dihydropyrazole
BRAF inhibitor

ABSTRACT

A series of novel 4,5-dihydropyrazole derivatives containing niacinamide moiety as potential V600E mutant BRAF kinase ($BRAF^{V600E}$) inhibitors were designed and synthesized. Results of the bioassays against $BRAF^{V600E}$ and WM266.4 human melanoma cell line showed several compounds to be endowed potent activities with IC_{50} and GI_{50} value in low micromolar range, among which compound **27e**, (5-(4-Chlorophenyl)-3-(4-methoxyphenyl)-4,5-dihydro-1*H*-pyrazol-1-yl)6-methylpyridin-3-yl methanone (IC_{50} = 0.20 μM, GI_{50} = 0.89 μM) was bearing the best bioactivity comparable with the positive control Sorafenib. Docking simulation was performed to determine the probable binding model and 3D-QSAR model was built to provide more pharmacophore understanding that could use to design new agents with more potent $BRAF^{V600E}$ inhibitory activity.

1. Introduction

The serine threonine kinase BRAF is a member of the RAF kinase family, which is part of the RAF/MEK/ERK serine threonine kinase cascade. This kinase cascade, also called the ERK/MAP kinase pathway (or 'classical' MAPK pathway), regulates cell growth, survival and differentiation,[1] and can be hyper-activated in approximately 30% of human cancers by many different membrane-bound receptors,[2] such as BRAF, the small G-proteins of the RAS family, and receptor tyrosine kinases. It has been reported that BRAF is mutated in many types of human tumors, most frequently observed in 50–70% of cell lines and tumors in melanoma, in 36–69% of papillary thyroid cancer, lower frequency in colorectal cancer (5–12%) and nonsmall cell lung cancer (1–4%). Approximately 90% of activating BRAF mutations in cancer lines are a glutamic acid to valine substitution at position 600 (V600E; formally identified as V599E).[3–7] In cancer cells, $BRAF^{V600E}$, ~500-fold more active than the wild-type protein,[8] stimulates constitutive ERK activity and drives proliferation and survival, thereby providing essential tumor growth and maintenance functions.[9] $BRAF^{V600E}$ also contributes to neoangiogenesis by stimulating vascular endothelial growth factor secretion.[10] Overall, these data suggest $BRAF^{V600E}$ as a therapeutic target[11] offering opportunities for anticancer drug development.

Inhibitors of BRAF have been developed, such as SB-590885,[12] sorafenib,[13] PLX4720,[14] and AZ628.[15] Among these inhibitors, SB-590885, one of the researching hot spots, is a novel triarylimidazole derivative, inhibits BRAF kinase activity with a K_i of 0.16 nmol/L, which is greater than 100-fold more potent than sorafenib. The origin of the selectivity of SB-590885 for BRAF seems to be due to interactions with several BRAF amino acids, as well as the presence of the indane-oxime. In particular, a phenylalanine residue (PHE583) in the COOH-terminal lobe forms favorable π-stacking interactions with the imidazole and pyridine rings of SB-590885.[12] Andrew K. also evaluated the SAR of a series of imidazole inhibitors based on SB-590885 targeting at BRAF kinase.[16] Lots of BRAF kinase inhibitors have been discovered with high-throughput screening of a chemical library and some structural modifications of the existing inhibitor scaffolds. But the inevitable high false positive proportion limits the application of virtual screen.

4,5-Dihydropyrazoles, an important class of heterocyclic small molecules, are important biological agents with a wide range of pharmaceutical (antitumor, anti-inflammatory, antifungal, antibacterial, and antiviral) and agrochemical activities.[17–19] Christopher et al. disclosed a 4,5-dihydropyrazole derivative as a potent, selective inhibitor of KSP (Kinesin spindle protein) to treat human cancer with good potency, pharmacokinetics and water solubility.[20] Havrylyuk et al. examined the in vitro anticancer activity of several novel thiazolone-based compounds containing

Abbreviations: BRAF, V-RAF murine sarcoma viral oncogene homolog B1; $BRAF^{V600E}$, V600E mutant BRAF; IC_{50}, half maximal inhibitory concentration; GI_{50}, the concentration that causes 50% growth inhibition; 3D-QSAR, quantitative structure–activity relationship.

* Corresponding author. Tel./fax: +86 25 83592672.
E-mail addresses: ghbxzh@yahoo.com.cn (H.-B. Gong), zhuhl@nju.edu.cn (H.-L. Zhu).

† Both authors contributed equally to the work.

0968-0896/$ - see front matter © 2012 Published by Elsevier Ltd.
http://dx.doi.org/10.1016/j.bmc.2012.04.047

the 5-aryl-3-phenyl-4,5-dihydro-1*H*-pyrazol-1-yl in the National Cancer Institute. Most of compounds displayed anticancer activity on leukemia, melanoma, lung, colon, CNS (central nervous system), ovarian, renal, prostate and breast cancer cell lines and the most efficient anticancer compound was found to be active with selective influence on colon cancer cell lines, especially on HT-29 ($\log GI_{50} = -6.37$).[21] Some dihydropyrazole derivatives used as potent and selective inhibitor of $BRAF^{V600E}$ with sound IC_{50} values have been identified by high-throughput screening.[22] Also, niacinamide (nicotinamide or nicotinic acid amide) is chemically known as pyridine-3-carboxamide, a form of vitamin B3, playing a significant role in cancer therapy. Niacinamide acts as a chemo- and radio-sensitizing agent, inhibits poly (ADP-ribose) polymerases (PARP-1), enzymes involved in the rejoining of DNA strand breaks induced by radiation or chemotherapy. Niacinamide is also used by some patients in combination with intravenous vitamin C therapy for cancer.[23] Based on the studies generalized above, a series of novel 4,5-dihydropyrazole derivatives containing

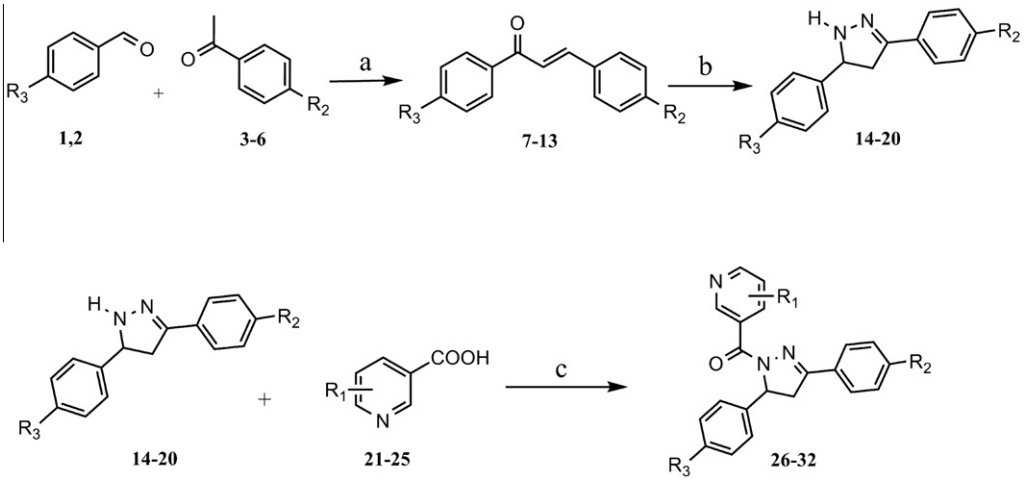

Scheme 1. Synthesis of compounds **1–35**. Reagents and conditions: (a) EtOH, rt; (b) $NH_2{\cdot}NH_2{\cdot}H_2O$, EtOH, reflux; (c) EDC·HCl, Cl_2H_2, reflux.

Table 1
Structural features, $BRAF^{V600E}$ inhibitory activity and antiproliferation activity of 35 compounds

Compound	R_1	R_2	R_3	IC_{50} (μM) $BRAF^{V600E}$	GI_{50} (μM) WM266.5
26a	5-Bromopyridin	4-OMe	4-OMe	4.58 ± 0.31	7.56 ± 0.43
26b	6-Chloropyridin	4-OMe	4-OMe	7.56 ± 1.23	6.45 ± 0.76
26c	2-Chloro-6-methylpyridin	4-OMe	4-OMe	5.14 ± 0.31	5.74 ± 0.51
26d	2-Chloropyridin	4-OMe	4-OMe	6.14 ± 0.37	4.35 ± 0.68
26e	6-Methylpyridin	4-OMe	4-OMe	3.42 ± 0.51	4.93 ± 0.61
27a	5-Bromopyridin	4-OMe	4-Cl	0.38 ± 0.04	1.29 ± 0.04
27b	6-Chloropyridin	4-OMe	4-Cl	0.51 ± 0.07	1.45 ± 0.05
27c	2-Chloro-6-methylpyridin	4-OMe	4-Cl	0.58 ± 0.04	1.44 ± 0.20
27d	2-Chloropyridin	4-OMe	4-Cl	0.47 ± 0.04	0.78 ± 0.06
27e	6-Methylpyridin	4-OMe	4-Cl	0.20 ± 0.03	0.89 ± 0.04
28a	5-Bromopyridin	4-OMe	4-Br	3.51 ± 0.39	5.63 ± 0.70
28b	6-Chloropyridin	4-OMe	4-Br	6.89 ± 0.50	7.13 ± 0.97
28c	2-Chloro-6-methylpyridin	4-OMe	4-Br	6.76 ± 0.46	8.47 ± 00.91
28d	2-Chloropyridin	4-OMe	4-Br	5.57 ± 0.43	3.05 ± 0.48
28e	6-Methylpyridin	4-OMe	4-Br	4.23 ± 0.33	4.28 ± 0.68
29a	5-Bromopyridin	4-OMe	4-Benzyloxy	4.27 ± 0.58	6.24 ± 0.89
29b	6-Chloropyridin	4-OMe	4-Benzyloxy	6.78 ± 0.41	10.64 ± 1.27
29c	2-Chloro-6-methylpyridin	4-OMe	4-Benzyloxy	3.01 ± 0.24	10.47 ± 1.45
29d	2-Chloropyridin	4-OMe	4-Benzyloxy	6.49 ± 0.47	9.15 ± 1.51
29e	6-Methylpyridin	4-OMe	4-Benzyloxy	1.63 ± 0.13	7.95 ± 1.31
30a	5-Bromopyridin	4-Cl	4-Benzyloxy	7.61 ± 0.42	8.13 ± 0.80
30b	6-Chloropyridin	4-Cl	4-Benzyloxy	16.43 ± 3.12	13.16 ± 2.81
30c	2-Chloro-6-methylpyridin	4-Cl	4-Benzyloxy	12.89 ± 1.89	11.36 ± 1.85
30d	2-Chloropyridin	4-Cl	4-Benzyloxy	4.42 ± 0.89	7.71 ± 0.99
30e	6-Methylpyridin	4-Cl	4-Benzyloxy	7.02 ± 0.61	9.20 ± 1.05
31a	5-Bromopyridin	4-Cl	4-Cl	4.77 ± 0.31	6.09 ± 1.22
31b	6-Chloropyridin	4-Cl	4-Cl	7.16 ± 0.77	9.89 ± 1.31
31c	2-Chloro-6-methylpyridin	4-Cl	4-Cl	7.77 ± 0.42	8.87 ± 1.05
31d	2-Chloropyridin	4-Cl	4-Cl	2.12 ± 0.34	3.58 ± 0.68
31e	6-Methylpyridin	4-Cl	4-Cl	3.58 ± 0.31	3.79 ± 0.88
32a	5-Bromopyridin	4-Cl	4-Br	7.82 ± 0.39	8.01 ± 1.00
32b	6-Chloropyridin	4-Cl	4-Br	7.34 ± 0.21	9.87 ± 1.52
32c	2-Chloro-6-methylpyridin	4-Cl	4-Br	7.35 ± 0.52	10.78 ± 1.36
32d	2-Chloropyridin	4-Cl	4-Br	8.67 ± 0.39	7.45 ± 1.26
32e	6-Methylpyridin	4-Cl	4-Br	7.05 ± 0.55	7.65 ± 0.78
Sorafenib				0.06	8.12

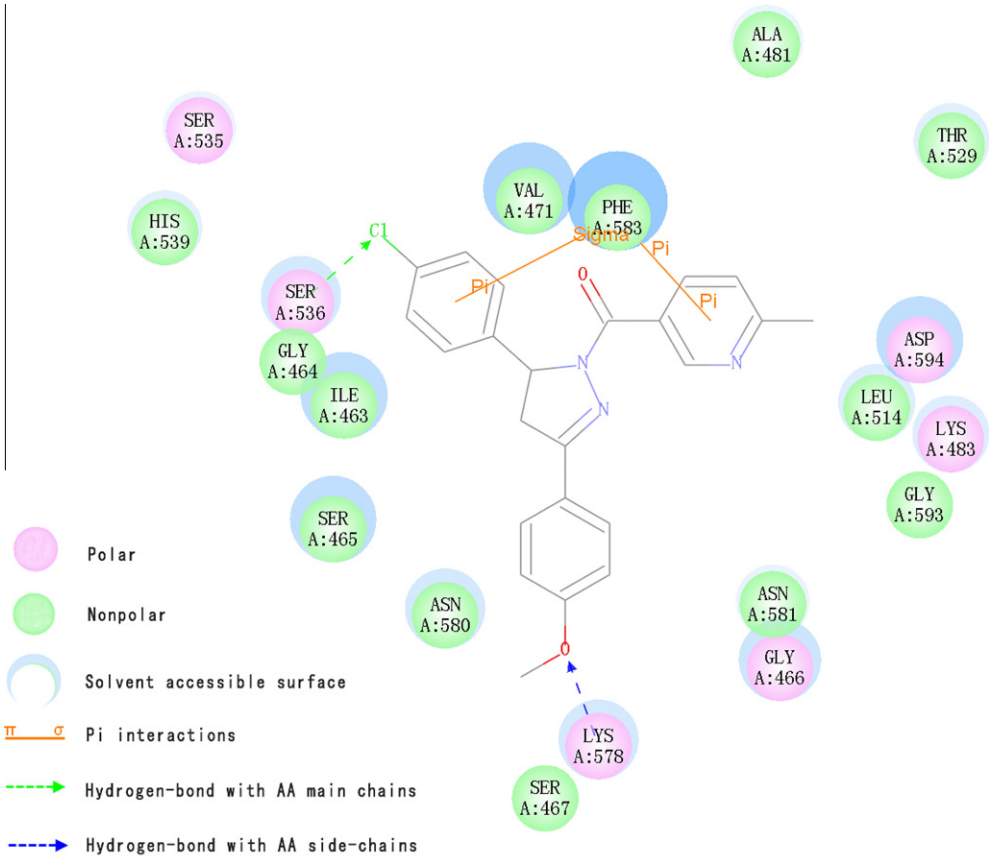

Figure 1. 2D diagram of binding model between BRAF and compound **27e**.

niacinamide moiety were designed as potential V600E mutant of BRAF kinase ($BRAF^{V600E}$) inhibitors and expected to have a sound cancer therapeutic benefit.

In this study, we describe the synthesis and the SAR of 4,5-dihydropyrazoles derivatives. Biological evaluation indicated that some of the synthesized compounds are potent inhibitors of $BRAF^{V600E}$. Docking simulations were performed using the X-ray crystallographic structure of the BRAF in complex with an inhibitor to explore the binding modes of these compounds at the active site. Based on the activity data, QSAR model was built to study the structure–activity relationship and guide the further study.

2. Results and discussion

2.1. Chemistry

The synthesis of 3,5-diphenyl-(4,5-dihydropyrazol-1-yl)pyridin-3-ylmethanones followed the general pathway outlined in Scheme 1. First of all, to a stirred solution of acetophenone derivative and benzaldehyde derivative in ethanol, KOH solution was added. The reaction mixture was stirred until the solids fully formed, and then obtained chalcones with yields of 90–95%. Next, treat chalcone derivatives in refluxing isopropanol with hydrazine hydrate for 8 h to get 3,5-diphenyl-4,5-dihydro-1*H*-pyrazoles. Finally, to a solution of 4,5-dihydropyrazole derivatives in dichloromethane, nicotinic acid derivatives was added, together with EDC (1-ethyl-3-(3-dimethylaminopropyl)carbodiimide) and HOBt (hydroxybenzotriazole). The mixture was refluxed under stirring for 8 h to give 3,5-diphenyl-(4,5-dihydropyrazol-1-yl) pyridin-3-yl methanones. All of the synthetic compounds gave satisfactory analytical and spectroscopic data, which were in full accordance with their depicted structures.

2.2. Bioassay

As described above, the $BRAF^{V600E}$ was considered as an important target for the development of small molecule inhibitors in the treatment of human cancers, particularly melanoma. The $BRAF^{V600E}$ inhibitory activities of the synthesized compounds were evaluated. The results, expressed as concentrations of IC_{50} (the half

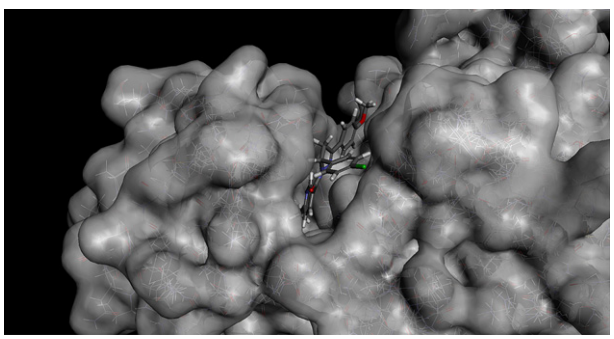

Figure 2. The receptor surface model with compounds **27e**.

maximal inhibitory concentration of $BRAF^{V600E}$ mediated MEK phosphorylation) and GI_{50} (the half maximal inhibitory concentration of WM266.4 human melanoma cell line growth), were summarized in Table 1 and revealed several significant points.

Among the synthesized 4,5-dihydropyrazole derivatives, analogs **26a–32e**, bearing the same core, showed a broad range of potencies, being compound **27e** the most potent agent with IC_{50} value of 0.20 μM and GI_{50} value of 0.89 μM, in contrast, compound **30b** exhibited a weak 16.43 μM IC_{50} value and 13.16 μM GI_{50} value.

Comprehensive study of the activity data shows that GI_{50} values of these compounds share a similar tendency with their relevant IC_{50} values. This relationship suggested the anti-proliferative effect was produced by inhibitory action against BRAF. In the series of 4,5-dihydropyrazole derivatives, the BRAF inhibitory activity of **26a–32e**, which were with different substituents on N-1 nitrogen atom of the 4,5-dihydropyrazole core, increased in the following order: Cl < Br < Me. Moreover analogs with 4-methoxyl substituent or 4-chloride substituent on 3-phenyl ring of 4,5-dihydropyrazole core exhibited thoroughly better activities of the former than the later. And replacement on 5-phenyl ring of 4,5-dihydropyrazole core results in a progressive potency, in order of 4-Cl < 4-Br < 4-benzyloxy < 4-OMe, as electronegativity decreases.

An acute oral toxicity test was conducted with rats to determine the toxicity from a single dose via the oral route. Based on the results of study (not listed), the single dose acute oral LD_{50} of the most potent compound, **27e** is greater than 5000 mg/kg of bodyweight.

2.3. Docking study

Molecular docking is an application wherein molecular modeling techniques are used to predict how a protein (enzyme) interacts with small molecules (ligands).[24] In the present study, to understand the interactions between compounds and BRAF and to explore their binding mode, a docking study was performed using the CDOCKER protocol in Discovery Studio 3.1 (Discovery Studio 3.1, Accelrys, Inc., San Diego, CA).

In the current study, we performed docking of thirty-five 4,5-dihydropyrazole derivatives into the active site of the receptor BRAF using CDOCKER in the Receptor–Ligand Interactions protocol section of Discovery Studio 3.1. The crystal structure of BRAF (PDB Code: 2FB8.pdb)[12] was obtained from the RCSB protein data bank (http://www.pdb.org). After preparing the receptor and ligands, the site sphere was selected based on the ligand binding location of SB-590885.

Binding model between the most potent compound **27e** with BRAF active site was showed in Figure 1 and Figure 2. In the binding model, compound **27e** is nicely bound to the active site of BRAF via hydrogen bond with SER536 (angle Cl···H–N = 169.4°, distance = 2.42 Å), LYS578 (angle O···H–N = 143.222°, distance = 1.84 Å), which proves compounds **27a–27e** substituted with 4-chloro on 5-phenyl ring and 4-methoxy on 3-phenyl ring of 4,5-dihydropyrazole core performs the most potent activity. Also PHE583 plays an important role in the complex involving π–π interactions (angle = 25.3°, distance = 5.42 Å) with the pyridin ring at the N1 atom and π–sigma interactions (distance = 6.02 Å) with the 5-phenyl ring of 4,5-dihydropyrazole core, which shares the same interaction method of SB-590885. The substitutional group also forms the hydrogen bond with BRAF. The only difference is that 4,5-dihydropyrazole core plays a structural role in the binding model.[12] The receptor surface model was showed in Figure 2, which revealed that the molecule occupies the ATP-binding pocket and binds to an active conformation of BRAF. The hydrophobic pocket including VAL471, PHE583, ALA481, THR529, LEU514 and ASN581 is occupied by niacinamide substituted with methyl. This binding model confirms the importance of hydrophobic group in niacinamide.

2.4. QSAR model

In order to give a systematic evaluation on 4,5-dihydropyrazole derivates as BRAF inhibitors and to explore more potent inhibitors, 3D-QSAR models were built using the creat 3D-QSAR protocol of Discovery Studio 3.1. In this study, 35 compounds bearing 4,5-dihydropyrazole core with definite IC_{50} values were selected as the model dataset. By convention, the pIC_{50} scale ($-\log IC_{50}$), in which higher values indicate exponentially greater potency, is used as a method to measure inhibitory activity. The training and test set was chosen by the Diverse Molecules method in Discovery Studio.

Considering a good alignment is very important for the analysis of molecular fields, the alignment conformation of each molecule was the one with lowest energy in the docked results of CDOCKER. And before building the QSAR model, we apply the alignment by the substructure (4,5-dihydro-1*H*-pyrazol-1-yl)methanone.

The correlation coefficient r^2 between observed and predicted activity of training set was found to be 0.736, while that of test set was found to be 0.789, which proves the QSAR model we built was acceptable. Predicted pIC_{50} values of 35 compounds by QSAR model we built have been given in Table 2. The well agreement between predicted pIC_{50} value and experimental pIC_{50} value for both test sets and training sets are shown in Figure 3.

Also the molecules aligned with the *iso*-surfaces of the 3D-QSAR model coefficients on electrostatic potential grids (Fig. 4a) and van

Table 2
Experimental, predicted inhibitory activity of compounds **26a**–**32e** by 3D-QSAR models based upon active conformation achieved by molecular docking

Compound	$BRAF^{V600E}$		Residual error
	Experimental pIC_{50}	Predicted pIC_{50}	
26a	5.339	5.400	−0.061
26b	5.121	5.390	−0.269
26c	5.289	5.330	−0.041
26d	5.212	5.285	−0.074
26e	5.466	5.478	−0.012
27a	6.420	6.000	0.421
27b	6.292	5.999	0.294
27c	6.237	6.117	0.119
27d	6.328	6.090	0.238
27e	6.796	6.267	0.529
28a	5.455	5.457	−0.002
28b	5.162	5.051	0.110
28c	5.170	5.676	−0.506
28d	5.254	5.728	−0.474
28e	5.373	5.259	0.114
29a	5.272	5.045	0.228
29b	5.369	5.277	0.092
29c	5.521	5.795	−0.273
29d	5.188	5.056	0.132
29e	5.788	5.705	0.083
30a	5.119	4.995	0.123
30b	4.784	4.779	0.005
30c	4.890	4.729	0.160
30d	5.355	5.347	0.008
30e	5.154	4.804	0.350
31a	5.321	5.559	−0.238
31b	5.145	5.315	−0.170
31c	5.110	5.397	−0.287
31d	5.672	5.559	0.113
31e	5.446	5.884	−0.438
32a	5.107	5.118	−0.011
32b	5.134	4.862	0.272
32c	5.134	5.121	0.013
32d	5.062	5.147	−0.085
32e	5.152	5.078	0.074

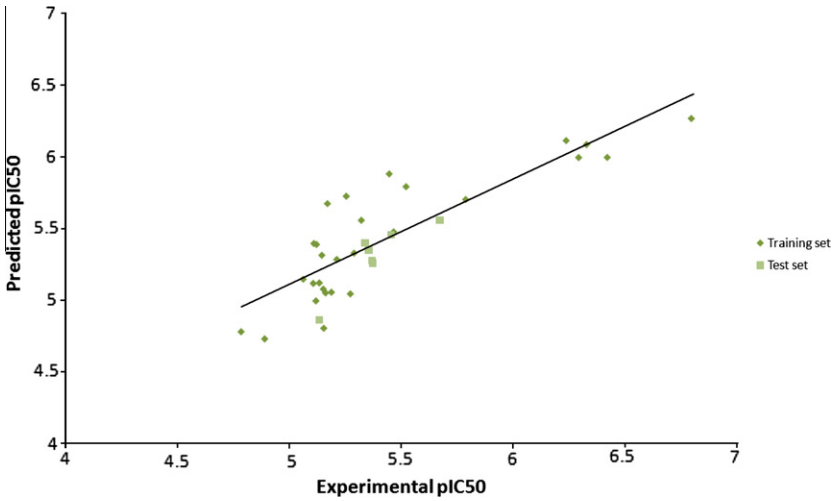

Figure 3. Plot of experimental versus predicted BRAF inhibitory activities of training set and test set.

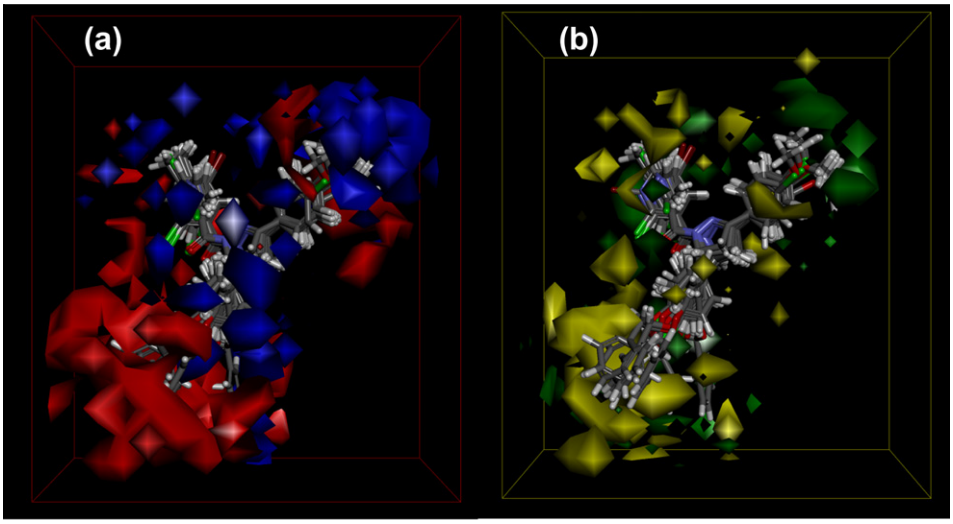

Figure 4. (a) 3D-QSAR model coefficients on electrostatic potential grids. Blue represents positive coefficients; red represents negative coefficients. (b) 3D-QSAR model coefficients on van der Waals grids. Green represents positive coefficients; yellow represents negative coefficients.

der Waals grids are listed (Fig. 4b). Electrostatic map indicates red contours around regions where high electron density (negative charge) is expected to increase activity, and blue contours represent areas where low electron density (partial positive charge) is expected to increase activity. Similarly, steric map indicates areas where steric bulk is predicted to increase (green) or decrease (yellow) activity. According to the maps, it suggested the compound with high negative charged and small R3 group, would show higher activity, validating that 4-Cl substituent being a better choice than 4-OMe. Whereas, a low negative charged and bulky R2 group would help obtain sound activity, validating the 4-OMe substituent could be more effective. As a result, data summarized above demonstrate that compounds **27e**, the most potent BRAF inhibitor (IC_{50} = 0.20 μM, GI_{50} = 0.89 μM), containing favor substituents has an outstanding activity.

3. Conclusion

In summary, a series of novel BRAF inhibitors containing 4,5-dihydropyrazole core was designed, prepared and tested for their inhibitory activity against BRAF. Results showed these compounds possessed potent antiproliferative activity against BRAF and WM266.4 human melanoma cell line, with IC_{50} and GI_{50} inhibitory values in low micromolar range. Among them, compound **27e** showed the most potent agent with IC_{50} value of 0.20 μM and GI_{50} value of 0.89 μM. The docking simulation was performed to get binding models and poses, and the result shows compound **27e** can bind well with the BRAF active site and act as BRAF inhibitor. QSAR model was also built by the activity data and binding conformations to provide a reliable tool for rational design of novel BRAF inhibitors.

4. Experimental section

4.1. Materials and measurements

All chemicals (reagent grade) used were commercially available. Separation of the compounds by column chromatography was carried out with silica gel 60 (200–300 mesh ASTM, E. Merck, Germany). The quantity of silica gel used was 50–100 times the weight charged on the column. Thin layer chromatography(TLC) was run on the silica gel coated aluminum sheets (silica gel 60 GF254, E.Merck, Germany) and visualized in ultraviolet (UV) light (254 nm). Developed plates were visualized by a Spectroline ENF

260C/F UV apparatus. Concentration and evaporation of the solvent after reaction or extraction were carried out on a rotary evaporator (Büchi Rotavapor) operating at reduced pressure. Melting points were measured on a Boetius micro melting point apparatus. All the Proton nuclear magnetic resonance (^{1}H NMR) and spectra were recorded on a DPX300 model Spectrometer at 25°C with TMS and solvent signals allotted as internal stands. Chemical shifts were reported in parts per million (d). ESI-MS spectra were recorded on a Mariner System 5304 Mass spectrometer. Elemental analyses were performed on a CHN-O-Rapid instrument and were within 0.4% of the theoretical values.

4.2. General procedure for synthesis of chalcones

To a stirred solution of acetophenone derivatives (1 mmol) and a benzaldehyde derivatives (1 mmol) in ethanol (30 mL), 6 M KOH (4 mL) was added and the reaction mixture was stirred until the solids fully formed. The products were filtrated and washed carefully with ice water and cool ethanol, and purified by crystallization from ethanol in refrigerator to give chalcones.

4.3. General method of synthesis of 3,5-diphenyl-4,5-dihydro-1*H*-pyrazole

To a solution of chalcone derivative (1 mmol) in isopropanol (5 mL) hydrazine hydrate (0.2 mL, 4 mmol) was added. The mixture was refluxed under stirring for 8 h, stored at 4–5 °C for 24 h, and the precipitate formed was filtered off, washed with cool ethanol. The synthesized compound was purified by crystallization from ethanol in refrigerator and allowed to air dry to give 4,5-dihydropyrazole derivatives.

4.4. General method of synthesis of (3,5-diphenyl-4,5-dihydropyrazol-1-yl) pyridine-3-yl methanone

To a solution of pyrazoline derivatives (1 mmol) in dichloromethane (5 mL) nicotinic acid derivatives (1 mmol) was added, together with EDC (1.2–1.5 mmol) and HOBt (1.2–1.5 mmol). The mixture was refluxed under stirring for 8 h. After completion of the reaction, the contents were cooled, and then evaporated to dryness in vacuo. Aqueous hydrochloric acid (0.1 M, 30 mL) was added and the mixture extracted with ethyl acetate (3 × 5 mL). The combined ethyl acetate layers were back-extracted with saturated sodium bicarbonate (1 × 5 mL) and brine (1 × 5 mL), dried over $MgSO_4$, filtered, and evaporated in vacuo. The residue was crystallized from ethanol to give target compounds **26a**–**32e**.

4.4.1. (3,5-Bis(4-methoxyphenyl)-4,5-dihydro-1*H*-pyrazol-1-yl)-5-bromopyridin-3-yl methanone (26a)

White powder, yield: 65%. Mp: 144–146 °C. ^{1}H NMR (300 MHz, $CDCl_3$, δ ppm): 3.23 (dd, J_1 = 4.77 Hz, J_2 = 17.73 Hz, 1H); 3.73–3.83 (m, 4H); 3.86 (s, 3H); 5.73 (dd, J_1 = 4.74 Hz, J_2 = 11.52 Hz, 1H); 6.86–6.96 (m, 4H); 7.24 (s, 2H); 7.67 (d, J = 8.76 Hz,2H); 8.46–8.75 (m, 2H); 9.20 (s, 1H). MS (ESI): 466.1 ([M+H]$^+$). Anal. Calcd for $C_{23}H_{20}BrN_3O_3$: C, 59.24; H, 4.32; N, 9.01%; Found: C, 59.46; H, 4.17; N, 9.28%.

4.4.2. (3,5-Bis(4-methoxyphenyl)-4,5-dihydro-1*H*-pyrazol-1-yl)-6-chloropyridin-3-yl methanone (26b)

Yellow powder, yield: 68%. Mp: 129–131 °C. ^{1}H NMR (300 MHz, $CDCl_3$, δ ppm): 3.19–3.27 (m, 1H); 3.73–3.82 (m, 4H); 3.86(s, 3H); 5.73 (dd, J_1 = 4.53 Hz, J_2 = 11.52 Hz, 1H); 6.86–6.95 (m, 5H); 7.25(s, 1H); 7.41 (d, J = 8.31 Hz, 1H); 7.67 (d, J = 8.70 Hz, 2H); 8.28 (d, J = 6.78 Hz,1H); 9.14 (s, 1H). MS (ESI): 422.1 ([M+H]$^+$). Anal. Calcd for $C_{23}H_{20}ClN_3O_3$: C, 65.48; H, 4.78; N, 9.96%; Found: C, 65.25; H, 4.99; N, 9.54%.

4.4.3. (3,5-Bis(4-methoxyphenyl)-4,5-dihydro-1*H*-pyrazol-1-yl)-2-chloro-6-methylpyridin-3-yl methanone (26c)

Yellow powder, yield: 61%. Mp: 161–163 °C. ^{1}H NMR (300 MHz, $CDCl_3$, δ ppm): 2.59 (s, 3H); 3.18–3.25 (m, 1H); 3.79–3.83 (m, 4H); 5.68 (dd, J_1 = 4.65 Hz, J_2 = 11.52 Hz, 1H); 6.86–6.90 (m, 4H); 7.14 (d, J = 7.68 Hz, 1H); 7.26–7.31 (m, 2H); 7.56 (d, J = 8.79 Hz, 2H); 7.66 (d, J = 7.68 Hz, 1H). MS (ESI): 436.1 ([M+H]$^+$). Anal. Calcd for $C_{24}H_{22}ClN_3O_3$: C, 66.13; H, 5.09; N, 9.64%; Found: C, 66.49; H, 5.21; N, 9.29%.

4.4.4. (3,5-Bis(4-methoxyphenyl)-4,5-dihydro-1*H*-pyrazol-1-yl)-2-chloropyridin-3-yl methanone (26d)

Brown powder, yield: 71%. Mp: 133–135 °C. ^{1}H NMR (300 MHz, $CDCl_3$, δ ppm): 3.19–3.27 (m, 1H); 3.80 (s, 3H); 3.82–3.85 (m, 4H); 5.67–5.72 (m, 1H); 6.86–6.91 (m, 4H); 7.23–7.32 (m, 3H); 7.55 (d, J = 8.94 Hz, 2H); 7.75–7.78 (m, 1H); 8.44–8.46 (m, 1H). MS (ESI): 422.1 ([M+H]$^+$). Anal. Calcd for $C_{23}H_{20}ClN_3O_3$: C, 65.48; H, 4.78; N, 9.96%; Found: C, 65.69; H, 4.59; N, 9.74%.

4.4.5. (3,5-Bis(4-methoxyphenyl)-4,5-dihydro-1*H*-pyrazol-1-yl)-6-methylpyridin-3-yl methanone (26e)

White powder, yield: 68%. Mp: 146–148 °C. ^{1}H NMR (300 MHz, $CDCl_3$, δ ppm): 2.56–2.67 (m, 3H); 3.19–3.27 (m, 1H); 3.76–3.91 (m, 3H); 3.84 (d, 4H); 5.70–5.76 (m, 1H); 6.87 (d, J = 8.40 Hz, 2H); 6.95–6.98 (m, 2H); 7.24 (s, 1H); 7.26–7.67 (m, 3H); 8.45–8.75 (m, 2H); 9.20 (s, 1H). MS (ESI): 402.2 ([M+H]$^+$). Anal. Calcd for $C_{24}H_{23}N_3O_3$: C, 71.80; H, 5.77; N, 10.47%; Found: C, 71.47; H, 5.59; N, 10.75%.

4.4.6. (5-(4-Chlorophenyl)-3-(4-methoxyphenyl)-4,5-dihydro-1*H*-pyrazol-1-yl) 5-bromopyridin-3-yl methanone (27a)

Yellow powder, yield: 79%. Mp: 148–150 °C. ^{1}H NMR (300 MHz, $CDCl_3$, δ ppm): 3.16–3.24 (m, 1H); 3.75–3.81 (m, 1H); 3.86 (s, 3H); 5.71–5.76(m, 1H); 6.94 (d, J = 8.97 Hz, 2H); 7.25–7.33 (m, 4H); 7.66 (d, J = 8.97 Hz, 2H); 8.46 (s, 1H); 8.76–8.77 (m, 1H); 9.21 (s, 1H). MS (ESI): 470.0 ([M+H]$^+$). Anal. Calcd for $C_{22}H_{17}BrClN_3O_2$:C, 56.13; H, 3.64; N, 8.93%; Found: C, 56.42; H, 3.46; N, 8.87%.

4.4.7. (5-(4-Chlorophenyl)-3-(4-methoxyphenyl)-4,5-dihydro-1*H*-pyrazol-1-yl)6-chloropyridin-3-yl methanone (27b)

Grey powder, yield: 65%. Mp: 174–176 °C. ^{1}H NMR (300 MHz, $CDCl_3$, δ ppm): 3.15–3.23 (m, 1H); 3.72–3.89 (m, 4H); 5.73–5.85 (m, 1H); 6.94 (d, J = 8.97 Hz, 2H); 7.26–7.34 (m, 4H); 7.40–7.42 (m, 1H); 7.64- 7.67 (m, 2H); 8.26–8.29 (m, 1H); 9.14 (s, 1H). MS (ESI): 426.1 ([M+H]$^+$). Anal. Calcd for $C_{22}H_{17}Cl_2N_3O_2$: C, 61.98; H, 4.02; N, 9.86%; Found: C, 61.59; H, 4.13; N, 9.59%.

4.4.8. (5-(4-Chlorophenyl)-3-(4-methoxyphenyl)-4,5-dihydro-1*H*-pyrazol-1-yl) 2-chloro-6-methylpyridin-3-yl methanone (27c)

Yellow powder, yield: 81%. Mp: 151–153 °C. ^{1}H NMR (300 MHz, $CDCl_3$, δ ppm): 2.62 (s, 3H); 3.17–3.25 (m, 1H); 3.79–3.89 (m, 4H); 5.63–5.72 (m, 1H); 6.70 (d, J = 8.76 Hz, 2H); 7.14–7.40 (m, 5H); 7.57 (d, J = 8.94 Hz, 2H); 7.68 (d, J = 7.68 Hz, 1H). MS (ESI): 440.1 ([M+H]$^+$). Anal. Calcd for $C_{23}H_{19}Cl_2N_3O_2$: C, 62.74; H, 4.35; N, 9.54%; Found: C, 62.55; H, 4.51; N, 9.36%.

4.4.9. (5-(4-Chlorophenyl)-3-(4-methoxyphenyl)-4,5-dihydro-1*H*-pyrazol-1-yl) 2-chloropyridin-3-yl methanone (27d)

Red powder, yield: 73%. Mp: 128–130 °C. ^{1}H NMR (300 MHz, $CDCl_3$, δ ppm): 3.17–3.25 (m, 1H); 3.79–3.89 (m, 4H); 5.70 (dd, J_1 = 4.74 Hz, J_2 = 11.52 Hz, 1H); 6.88 (d, J = 7.68 Hz, 2H); 7.31–7.43(m, 4H); 7.54 (d, J = 8.43 Hz, 2H); 7.77 (d, J = 8.87 Hz, 1H); 7.91–7.94 (m, 2H). MS (ESI): 426.1 ([M+H]$^+$). Anal. Calcd for $C_{22}H_{17}Cl_2N_3O_2$: C, 61.98; H, 4.02; N, 9.86%; Found: C, 61.73; H, 4.21; N, 9.55%.

4.4.10. (5-(4-Chlorophenyl)-3-(4-methoxyphenyl)-4,5-dihydro-1*H*-pyrazol-1-yl)6-methylpyridin-3-yl methanone (27e)

Yellow powder, yield: 75%. Mp: 161–163 °C. ^{1}H NMR (300 MHz, $CDCl_3$, δ ppm): 2.63 (s, 3H); 3.13–3.20 (m, 1H); 3.73–3.85 (m, 4H); 5.72–5.78 (m, 1H); 6.81 (d, J = 8.79 Hz, 1H); 6.93 (d, J = 8.79 Hz, 2H); 7.28–7.33 (m, 3H); 7.61–7.69 (m, 3H); 8.20–8.22 (m, 1H); 9.25 (s, 1H). MS (ESI): 406.1 ([M+H]$^+$). Anal. Calcd for $C_{23}H_{20}ClN_3O_2$: C, 68.06; H, 4.97; N, 10.35%; Found: C, 68.32; H, 4.79; N, 10.43%.

4.4.11. (5-(4-Bromophenyl)-3-(4-methoxyphenyl)-4,5-dihydro-1*H*-pyrazol-1-yl)5-bromopyridin-3-yl methanone (28a)

Yellow powder, yield: 61%. Mp: 170–172 °C. ^{1}H NMR (300 MHz, $CDCl_3$, δ ppm): 3.17–3.24 (m, 1H); 3.77–3.83 (m, 1H); 3.87 (s, 3H); 5.70–5.76 (m, 1H); 6.95 (d, J = 8.67 Hz, 2H); 7.20–7.22 (m, 2H); 7.49 (d, J = 8.31 Hz, 2H); 7.61–7.68 (m, 2H); 8.47 (s, 1H); 8.77 (s, 1H); 9.22 (s, 1H). MS (ESI): 514.0 ([M+H]$^+$). Anal. Calcd for $C_{22}H_{17}Br_2N_3O_2$: C, 51.29; H, 3.33; N, 8.16%; Found: C, 51.43; H, 3.17; N, 8.23%.

4.4.12. (5-(4-Bromophenyl)-3-(4-methoxyphenyl)-4,5-dihydro-1*H*-pyrazol-1-yl)6-chloropyridin-3-yl methanone (28b)

Yellow powder, yield: 74%. Mp: 190–192 °C. ^{1}H NMR (300 MHz, $CDCl_3$, δ ppm): 3.16–3.23 (m, 1H); 3.76–3.82 m, 1H); 3.87 (s, 3H); 5.70–5.75 (m, 1H); 6.94 (d, J = 8.70 Hz, 2H); 7.20–7.22 (m, 2H); 7.41–7.50 (m, 3H); 7.66 (d, J = 6.42 Hz, 2H); 8.28 (s, 1H); 9.15 (s, 1H). MS (ESI): 470.0 ([M+H]$^+$). Anal. Calcd for $C_{22}H_{17}BrClN_3O_2$: C, 56.13; H, 3.64; N, 8.93%; Found: C, 56.35; H, 3.48; N, 8.85%.

4.4.13. (5-(4-Bromophenyl)-3-(4-methoxyphenyl)-4,5-dihydro-1*H*-pyrazol-1-yl)2-chloro-6-methylpyridin-3-yl methanone (28c)

Yellow powder, yield: 78%. Mp: 159–161 °C. ^{1}H NMR (300 MHz, $CDCl_3$, δ ppm): 2.60 (s, 3H); 3.15–3.23 (m, 1H); 3.77–3.87 (m, 4H); 5.65–5.70 (m, 1H); 6.88 (d, J = 8.94 Hz, 2H); 7.16 (d, J = 7.68 Hz, 1H); 7.24 (s, 1H); 7.26 (s, 1H); 7.48–7.51 (m, 2H); 7.55 (d, J = 8.97 Hz, 2H); 7.66 (d, J = 7.68 Hz, 1H). MS (ESI): 484.0 ([M+H]$^+$). Anal. Calcd for $C_{23}H_{19}BrClN_3O_2$: C, 56.98; H, 3.95; N, 8.67%; Found: C, 56.64; H, 3.78; N, 8.72%.

4.4.14. (5-(4-Bromophenyl)-3-(4-methoxyphenyl)-4,5-dihydro-1*H*-pyrazol-1-yl)2-chloropyridin-3-yl methanone (28d)

Yellow powder, yield: 75%. Mp: 139–141 °C. ^{1}H NMR (300 MHz, $CDCl_3$, δ ppm): 3.17–3.24 (m, 1H); 3.79–3.88 (m, 4H); 5.69 (dd, J_1 = 4.77 Hz, J_2 = 11.52 Hz, 1H); 6.87 (d, J = 8.43 Hz, 2H); 7.25–7.26 (m, 1H); 7.28 (s, 1H); 7.30–7.34 (m, 1H); 7.49–7.55 (m, 4H); 7.77 (dd, J_1 = 2.01 Hz, J_2 = 7.50 Hz, 1H); 8.46–8.48 (m, 1H). MS (ESI): 470.0 ([M+H]$^+$). Anal. Calcd for $C_{22}H_{17}BrClN_3O_2$: C, 56.13; H, 3.64; N, 8.93%; Found: C, 56.41; H, 3.48; N, 8.86%.

4.4.15. (5-(4-Bromophenyl)-3-(4-methoxyphenyl)-4,5-dihydro-1*H*-pyrazol-1-yl)6-methylpyridin-3-yl methanone (28e)

Grey powder, yield: 71%. Mp: 139–141 °C. ^{1}H NMR (300 MHz, $CDCl_3$, δ ppm): 2.64 (s, 3H); 3.17–3.24 (m, 1H); 3.85–3.89 (m, 4H); 6.75 (s, 1H); 7.50–7.57 (m, 3H); 7.60–7.63 (m, 2H); 7.70–7.76 (m, 1H); 7.84 (d, J = 8.76 Hz, 2H); 7.96–7.99 (m, 2H); 8.03 (d, J = 8.94 Hz, 1H). MS (ESI): 450.1([M+H]$^+$). Anal. Calcd for $C_{23}H_{20}BrN_3O_2$: C, 61.34; H, 4.48; N, 9.33%; Found: C, 61.61; H, 4.54; N, 9.59%.

4.4.16. (5-(4-(Benzyloxy)phenyl)-3-(4-methoxyphenyl)-4,5-dihydro-1*H*-pyrazol-1-yl)5-bromopyridin-3-yl methanone (29a)

Yellow powder, yield: 63%. Mp: 106–108 °C. ^{1}H NMR (300 MHz, $CDCl_3$, δ ppm): 3.20–3.27 (m, 1H); 3.78 (dd, J_1 = 11.52 Hz, J_2 = 17.76 Hz, 1H); 3.86 (s, 3H); 5.04 (s, 2H); 5.71–5.76 (m, 1H); 6.93–6.96 (m, 5H); 7.26 (d, J = 6.03 Hz, 1H); 7.31–7.40 (m, 5H); 7.67 (d, J = 8.67 Hz, 2H); 8.47 (s, 1H); 8.76 (s, 1H); 9.21 (s, 1H). MS (ESI): 542.1 ([M+H]$^+$). Anal. Calcd for $C_{29}H_{24}BrN_3O_3$: C, 64.21; H, 4.46; N, 7.75%; Found: C, 64.40; H, 4.62; N, 7.48%.

4.4.17. (5-(4-(Benzyloxy)phenyl)-3-(4-methoxyphenyl)-4,5-dihydro-1*H*-pyrazol-1-yl)6-chloropyridin-3-yl methanone (29b)

Yellow powder, yield: 75%. Mp: 144–147 °C. ^{1}H NMR (300 MHz, $CDCl_3$, δ ppm): 3.23 (dd, J_1 = 4.53 Hz, J_2 = 17.73 Hz, 1H); 3.72–3.82(m, 1H; 3.86 (s, 3H); 5.04 (s, 2H); 5.73 (dd, J_1 = 4.53 Hz, J_2 = 11.34 Hz, 1H); 6.93–6.96 (m, 4H); 7.26 (d, J = 6.03 Hz, 1H); 7.35–7.42 (m, 7H); 7.67 (d, J = 8.49 Hz, 2H); 8.28 (d, J = 6.42 Hz, 1H); 9.14 (s, 1H). MS (ESI): 498.2 ([M+H]$^+$). Anal. Calcd for $C_{29}H_{24}ClN_3O_3$: C, 69.95; H, 4.86; N, 8.44%; Found: C, 69.59; H, 4.69; N, 8.27%.

4.4.18. (5-(4-(Benzyloxy)phenyl)-3-(4-methoxyphenyl)-4,5-dihydro-1*H*-pyrazol-1-yl)2-chloro-6-methylpyridin-3-yl methanone (29c)

Yellow powder, yield: 79%. Mp: 207–209 °C. ^{1}H NMR (300 MHz, $CDCl_3$, δ ppm): 2.60 (s, 3H); 3.20–3.25 (m, 1H); 3.74–3.82 (m, 4H); 5.04 (s, 2H); 5.66–5.71 (m, 1H); 6.86–6.89 (m, 2H); 6.95–6.98 (m, 2H); 7.15 (d, J = 7.68 Hz,1H); 7.28–7.33 (m, 3H); 7.35–7.43 (m, 4H); 7.56 (d, J = 8.58 Hz, 2H); 7.66 (d, J = 7.68 Hz,1H). MS (ESI): 512.2([M+H]$^+$). Anal. Calcd for $C_{30}H_{26}ClN_3O_3$: C, 70.38; H, 5.12; N, 8.21%; Found: C, 70.52; H, 5.31; N, 8.46%.

4.4.19. (5-(4-(Benzyloxy)phenyl)-3-(4-methoxyphenyl)-4,5-dihydro-1*H*-pyrazol-1-yl)2-chloropyridin-3-yl methanone (29d)

Brown powder, yield: 64%. Mp: 146–147 °C. ^{1}H NMR (300 MHz, $CDCl_3$, δ ppm): 3.23 (dd, J_1 = 4.56 Hz, J_2 = 17.55 Hz, 1H); 3.75–3.85 (m, 4H); 5.05 (s, 2H); 5.70 (dd, J_1 = 4.38 Hz, J_2 = 11.52 Hz, 1H); 6.87 (d, J = 8.58 Hz, 2H); 6.97 (d, J = 8.79 Hz, 2H); 7.29–7.34 (m, 4H); 7.35–7.43 (m, 4H); 7.53–7.60 (m, 2H); 7.77 (dd, J_1 = 1.83 Hz, J_2 = 7.5 Hz, 1H); 8.44–8.47 (m, 1H). MS (ESI): 598.2 ([M+H]$^+$). Anal. Calcd for $C_{29}H_{24}ClN_3O_3$: C, 69.95; H, 4.86; N, 8.44%; Found: C, 69.59; H, 4.69; N, 8.63%.

4.4.20. (5-(4-(Benzyloxy)phenyl)-3-(4-methoxyphenyl)-4,5-dihydro-1*H*-pyrazol-1-yl)6-methylpyridin-3-yl methanone (29e)

Grey powder, yield: 69%. Mp: 108–110 °C. ^{1}H NMR (300 MHz, $CDCl_3$, δ ppm): 2.56 (s, 3H); 3.13–3.27 (m, 1H); 3.85–3.89 (m, 4H); 5.03–5.15 (m, 2H); 5.70–5.79 (m, 1H); 6.96–7.06 (m, 4H); 7.34–7.45 (m, 7H); 7.60 (d, J = 8.79 Hz, 2H); 7.77 (d, J = 15.54 Hz, 1H); 8.02–8.04 (m, 2H). MS (ESI): 478.2 ([M+H]$^+$). Anal. Calcd for $C_{30}H_{27}N_3O_3$: C, 75.45; H, 5.70; N, 8.80%; Found: C, 75.67; H, 5.55; N, 8.48%.

4.4.21(5-(4-(Benzyloxy)phenyl)-3-(4-chlorophenyl)-4,5-dihydro-1*H*-pyrazol-1-yl)5-bromopyridin-3-yl methanone (30a)

White powder, yield: 73%. Mp: 129–131 °C. ^{1}H NMR (300 MHz, $CDCl_3$, δ ppm): 3.14–3.23 (m, 1H); 3.78–3.83 (m, 1H); 5.06 (s, 2H); 5.71–5.83 (m, 1H); 6.75 (s, 1H); 6.99 (d, J = 8.58 Hz , 3H); 7.49–7.57 (m, 3H); 7.62 (d, J = 8.97 Hz, 2H); 7.7–7.79 (m, 1H); 7.84 (d, J = 8.83 Hz, 2H); 7.97–8.03 (m, 3H); 9.23–9.25 (m, 1H). MS (ESI): 546.1 ([M+H]$^+$). Anal. Calcd for $C_{28}H_{21}BrClN_3O_2$: C, 61.50; H, 3.87; N, 7.68%; Found: C, 61.73; H, 3.75; N, 7.93%.

4.4.22(5-(4-(Benzyloxy)phenyl)-3-(4-chlorophenyl)-4,5-dihydro-1*H*-pyrazol-1-yl)6-chloropyridin-3-yl methanone (30b)

Yellow powder, yield: 71%. Mp: 154–156 °C. ^{1}H NMR (300 MHz, $CDCl_3$, δ ppm): 3.19–3.27 (m, 1H); 3.73–3.83 (m, 1H); 5.04 (s, 2H); 5.73–5.79 (m, 1H); 6.91–6.97 (m, 2H); 7.24 (d, J = 9.33 Hz , 2H); 7.31–7.42 (m, 4H); 7.46–7.51 (m, 3H) 7.61–7.66 (m, 3H); 8.24 (d, J = 6.24 Hz ,1H); 9.10 (s, 1H). MS (ESI): 502.1 ([M+H]$^+$). Anal. Calcd for $C_{28}H_{21}Cl_2N_3O_2$: C, 66.94; H, 4.21; N, 8.36%; Found: C, 66.58; H, 4.40; N, 8.52%.

4.4.23.(5-(4-(Benzyloxy)phenyl)-3-(4-chlorophenyl)-4,5-dihydro-1*H*-pyrazol-1-yl)2-chloro-6-methylpyridin-3-yl methanone (30c)

Orange powder, yield: 78%. Mp: 161–163 °C. ^{1}H NMR (300 MHz, $CDCl_3$, δ ppm): 2.61 (s, 3H); 3.23 (d, J = 17.73 Hz ,1H); 3.71–3.85 (m, 1H); 5.04 (d, J = 8.25 Hz ,2H); 5.71 (d, J = 6.75 Hz ,1H); 6.97 (d, J = 8.43 Hz ,2H); 7.15–7.17 (m, 1H); 7.28–7.43 (m, 9H); 7.52 (d, J = 8.40 Hz ,2H); 7.65–7.68 (m, 1H). MS (ESI): 516.1 ([M+H]$^+$). Anal. Calcd for $C_{29}H_{23}Cl_2N_3O_2$: C, 67.45; H, 4.49; N, 8.14%; Found: C, 67.65; H, 4.69; N, 8.34%.

4.4.24(5-(4-(Benzyloxy)phenyl)-3-(4-chlorophenyl)-4,5-dihydro-1*H*-pyrazol-1-yl)2-chloropyridin-3-yl methanone (30d)

Brown powder, yield: 74%. Mp: 162–164 °C. ^{1}H NMR (300 MHz, $CDCl_3$, δ ppm): 3.24 (dd, J_1 = 4.74 Hz, J_2 = 17.73 Hz, 1H); 3.75–3.86 (m, 1H); 5.06 (s, 2H); 5.69–5.75 (m, 1H); 6.98 (d, J = 8.79 Hz , 2H); 7.28–7.32 (m, 4H); 7.35–7.44 (m, 3H); 7.47–7.51 (m, 3H) 7.53 (d, J = 8.61 Hz , 2H); 7.75–7.78 (m, 1H); 8.46–8.48 (m, 1H). MS (ESI): 502.1 ([M+H]$^+$). Anal. Calcd for $C_{28}H_{21}Cl_2N_3O_2$: C, 66.94; H, 4.21; N, 8.36%; Found: C, 66.73; H, 4.40; N, 8.01%.

4.4.25(5-(4-(Benzyloxy)phenyl)-3-(4-chlorophenyl)-4,5-dihydro-1*H*-pyrazol-1-yl)6-methylpyridin-3-yl methanone (30e)

White powder, yield: 69%. Mp: 115–117 °C. ^{1}H NMR (300 MHz, $CDCl_3$, δ ppm): 2.64 (s, 3H); 3.21–3.25 (m, 1H); 3.74–3.81 (m, 1H); 5.16 (s, 2H); 6.76 (m, 1H); 7.02–7.09 (m, 2H); 7.23–7.30 (m, 4H); 7.34–7.47 (m, 4H); 7.62–7.65 (m, 2H); 7.81 (d, J = 8.79 Hz, 1H); 7.91–8.00 (m, 2H); 8.67(s, 1H). MS (ESI): 482.2([M+H]$^+$). Anal. Calcd for $C_{29}H_{24}ClN_3O_2$: C, 72.27; H, 5.02; N, 8.72%; Found: C, 72.52; H, 5.19; N, 8.54%.

4.4.26. (3,5-Bis(4-chlorophenyl)-4,5-dihydro-1*H*-pyrazol-1-yl)5-bromopyridin-3-yl methanone (31a)

White powder, yield: 78%. Mp: 143–145 °C. ^{1}H NMR (300 MHz, $CDCl_3$, δ ppm): 3.17–3.24 (m, 1H); 3.77–3.87 (m, 1H); 5.74–5.79 (m, 1H); 7.24–7.27 (m, 2H); 7.34 (d, J = 8.61 Hz, 2H); 7.41 (d, J = 8.40 Hz, 2H); 7.64 (d, J = 8.61 Hz, 2H); 8.42 (s, 1H); 8.77–8.78 (m, 1H); 9.18 (s, 1H). MS (ESI): 474.0 ([M+H]$^+$). Anal. Calcd for $C_{21}H_{14}BrCl_2N_3O$: C, 53.08; H, 2.97; N, 8.84%; Found: C, 53.32; H, 2.84; N, 8.79%.

4.4.27. (3,5-Bis(4-chlorophenyl)-4,5-dihydro-1*H*-pyrazol-1-yl)6-chloropyridin-3-yl methanone(31b)

White powder, yield: 79%. Mp: 178–180 °C. ^{1}H NMR (300 MHz, $CDCl_3$, δ ppm): 3.18–3.26 (m, 1H); 3.78–3.88 (m, 1H); 5.78 (dd, J_1 = 5.13 Hz, J_2 = 11.70 Hz, 1H); 7.26 (s, 1H); 7.28 (d, J = 2.19 Hz, 1H); 7.35 (d, J = 8.40 Hz, 2H); 7.41–7.46 (m, 3H); 7.65 (dd, J_1 = 1.83 Hz, J_2 = 6.78 Hz, 2H); 8.24–8.28 (m, 1H); 9.13 (s, 1H). MS (ESI): 430.0([M+H]$^+$). Anal. Calcd for $C_{21}H_{14}Cl_3N_3O$: C, 58.56; H, 3.28; N, 9.76%; Found: C, 58.34; H, 3.32; N, 9.45%.

4.4.28. (3,5-Bis(4-chlorophenyl)-4,5-dihydro-1*H*-pyrazol-1-yl)2-chloro-6-methylpyridin-3-yl methanone (31c)

White powder, yield: 63%. Mp: 187–189 °C. ^{1}H NMR (300 MHz, $CDCl_3$, δ ppm): 2.65 (m, 3H); 3.78–3.83 (m, 1H); 3.96–4.06 (m, 1H); 5.72–5.81 (m, 1H); 7.16 (d, 2H); 7.29–7.32 (m, 2H); 7.39 (d, J = 8.40 Hz, 3H); 7.78 (d, J = 8.04 Hz, 3H). MS (ESI): 444.0 ([M+H]$^+$). Anal. Calcd for $C_{22}H_{16}Cl_3N_3O$: C, 59.41; H, 3.63; N, 9.45%; Found: C, 59.63; H, 3.44; N, 9.78%.

4.4.29. (3,5-Bis(4-chlorophenyl)-4,5-dihydro-1*H*-pyrazol-1-yl)2-chloropyridin-3-yl methanone (31d)

White powder, yield: 66%. Mp: 178–180 °C. ^{1}H NMR (300 MHz, $CDCl_3$, δ ppm): 2.94 (s, 1H); 3.99–4.03 (m, 1H); 5.67–5.79 (m, 1H); 7.16 (d, J = 8.40 Hz, 2H); 7.29–7.32 (m, 3H); 7.38 (d, J = 7.86 Hz, 3H); 7.68 (s, 3H). MS (ESI): 430.0([M+H]$^+$). Anal. Calcd for $C_{21}H_{14}Cl_3N_3O$: C, 58.56; H, 3.28; N, 9.76%; Found: C, 58.82; H, 3.41; N, 9.39%.

4.4.30. (3,5-Bis(4-chlorophenyl)-4,5-dihydro-1*H*-pyrazol-1-yl)6-methylpyridin-3-yl methanone (31e)

White powder, yield: 65%. Mp: 146–148 °C. ^{1}H NMR (300 MHz, $CDCl_3$, δ ppm): 2.68 (s, 3H); 3.18–3.25 (m, 1H); 3.88–3.92 (m, 1H); 5.56–5.69 (m, 1H); 6.79 (s, 1H); 7.43–7.50 (m, 5H); 7.94 (d, J = 8.61 Hz, 2H); 7.99–8.05 (m, 2H); 8.56 (s, 1H). MS (ESI): 410.1([M+H]$^+$). Anal. Calcd for $C_{22}H_{17}Cl_2N_3O$: C, 64.40; H, 4.18; N, 10.24%; Found: C, 64.71; H, 4.09; N, 10.52%.

4.4.31. (5-(4-Bromophenyl)-3-(4-chlorophenyl)-4,5-dihydro-1*H*-pyrazol-1-yl)5-bromopyridin-3-yl methanone (32a)

Pink powder, yield: 63%. Mp: 156–158 °C. ^{1}H NMR (300 MHz, $CDCl_3$, δ ppm): 3.18–3.26 (m, 1H); 3.79–3.88 (m, 1H); 5.77 (dd, J_1 = 4.95 Hz, J_2 = 11.70 Hz, 1H); 7.21 (d, J = 8.22 Hz, 2H); 7.43 (d, J = 8.58 Hz, 2H); 7.51–7.66 (m, 4H); 8.44 (s, 1H); 8.79 (s, 1H); 9.20 (s, 1H). MS (ESI): 517.9 ([M+H]$^+$). Anal. Calcd for $C_{21}H_{14}Br_2ClN_3O$: C, 48.54; H, 2.72; N, 8.09%; Found: C, 48.63; H, 2.68; N, 8.41%.

4.4.32. (5-(4-Bromophenyl)-3-(4-chlorophenyl)-4,5-dihydro-1*H*-pyrazol-1-yl)6-chloropyridin-3-yl methanone (32b)

White powder, yield: 68%. Mp: 175–178 °C. ^{1}H NMR (300 MHz, $CDCl_3$, δ ppm): 3.21 (dd, J_1 = 5.13 Hz, J_2 = 17.91 Hz, 1H); 3.78–3.88 (m, 1H); 5.74–5.80 (m, 1H); 7.21 (d, J = 8.40 Hz, 2H); 7.41–7.46 (m, 3H); 7.49–7.59 (m, 2H); 7.66 (d, J = 8.40 Hz, 2H); 8.24–8.38 (m, 1H); 9.11–9.13 (m, 1H). MS (ESI): 474.0 ([M+H]$^+$). Anal. Calcd for $C_{21}H_{14}BrCl_2N_3O$: C, 53.08; H, 2.97; N, 8.84%; Found: C, 53.32; H, 2.76; N, 8.71%.

4.4.33. (5-(4-Bromophenyl)-3-(4-chlorophenyl)-4,5-dihydro-1*H*-pyrazol-1-yl2-chloro-6-methylpyridin-3-yl methanone (32c)

Yellow powder, yield: 75%. Mp: 153–155 °C. ^{1}H NMR (300 MHz, $CDCl_3$, δ ppm): 2.65 (s, 3H); 3.78–2.87 (m, 1H); 3.94–4.09 (m, 1H); 5.73–5.85 (m, 1H); 7.19 (d, J = 7.68 Hz, 2H); 7.39–7.42 (m, 2H); 7.39–7.45 (m, 3H); 7.78–7.89 (m, 2H); 8.14–8.21 (m, 1H). MS (ESI): 488.0 ([M+H]$^+$). Anal. Calcd for $C_{22}H_{16}BrCl_2N_3O$: C, 54.01; H, 3.30; N, 8.59%; Found: C, 54.22; H, 3.25; N, 8.90%.

4.4.34. (5-(4-Bromophenyl)-3-(4-chlorophenyl)-4,5-dihydro-1*H*-pyrazol-1-yl)2-chloropyridin-3-yl methanone (32d)

Grey powder, yield: 73%. Mp: 158–160 °C. ^{1}H NMR (300 MHz, $CDCl_3$, δ ppm): 3.19–3.27 (m, 1H); 3.73–3.79 (m, 1H); 5.72–5.83 (m, 1H); 7.29–7.33 (m, 2H); 7.53–7.57 (m, 2H); 7.75 (d, J = 8.45 Hz ,1H); 7.83–8.77 (m, 3H); 7.94 (dd, J_1 = 8.58 Hz, J_2 = 11.52 Hz, 2H); 8.23–8.27 (m, 1H). MS (ESI): 474.0 ([M+H]$^+$). Anal. Calcd for $C_{21}H_{14}BrCl_2N_3O$: C, 53.08; H, 2.97; N, 8.84%; Found: C, 53.21; H, 2.79; N, 8.76%.

4.4.35. (5-(4-Bromophenyl)-3-(4-chlorophenyl)-4,5-dihydro-1*H*-pyrazol-1-yl) 6-methylpyridin-3-yl methanone (32e)

White powder, yield: 65%. Mp: 154–156 °C. ^{1}H NMR (300 MHz, $CDCl_3$, δ ppm): 2.63 (s, 3H); 3.15–3.25 (m, 1H); 3.89–3.93 (m, 1H); 5.58–5.67 (m, 1H); 6.79–6.83 (m, 1H); 7.47–7.56 (m, 4H); 7.67–7.89 (m, 3H); 7.94 (d, J = 8.79 Hz ,2H); 8.12–8.20 (m, 1H). MS (ESI): 453.0([M+H]$^+$). Anal. Calcd for $C_{22}H_{17}BrClN_3O$: C, 58.11; H, 3.77; N, 9.24%; Found: C, 58.43; H, 3.69; N, 9.45%.

4.5. Antiproliferative activity

WM266.5 melanoma cells were cultured in DMEM/10% fetal bovine serum, in 5% CO_2 water saturated atmosphere at 37 °C. Cell suspensions (10000/mL) were prepared and 100 μL/well dispensed

into 96-well plates (Costar) giving 1000 cells/well. The plates were returned to the incubator for 24 h to allow the cells to reattach. These compounds were initially prepared at 20 mM in DMSO. Aliquots (200 μL) were diluted into 20 mL culture medium giving 200 μM, and 10 serial dilutions of 3× prepared. Aliquots (100 μL) of each dilution were added to the wells, giving doses ranging from 100 μM–0.005 μM. After a further incubated at 37 °C for 24 h in a humidified atmosphere with 5% CO_2, the cell viability was assessed by the conventional 3-(4,5-dimethylthiazol-2-yl)-2,5-diphenyltetrazolium bromide (MTT) reduction assay and carried out strictly according to the manufacturer instructions (Sigma). The absorbance at 590 nm was recorded using LX300 Epson Diagnostic microplate reader. Then GI_{50} was calculated using SPSS 13.0 software.

4.6. Kinase Assay

This V600E mutant BRAF kinase assay was performed in triplicate for each tested compound in this study. Briefly, 7.5 ng Mouse Full-Length GST-tagged $BRAF^{V600E}$ (Invitrogen, PV3849) was preincubated at room temperature for 1 h with 1 μL drug and 4 μL assay dilution buffer. The kinase assay was initiated when 5 μL of a solution containing 200 ng recombinant human full length, N-terminal His-tagged MEK1 (Invitrogen), 200 μM ATP, and 30 mM $MgCl_2$ in assay dilution buffer was added. The kinase reaction was allowed to continue at room temperature for 25 min and was then quenched with 5 μL 5× protein denaturing buffer (LDS) solution. Protein was further denatured by heating for 5 min at 70 °C. 10 μL of each reaction was loaded into a 15-well, 4–12% precast NuPage gel (Invitrogen) and run at 200 V, and upon completion, the front, which contained excess hot ATP, was cut from the gel and discarded. The gel was then dried and developed onto a phosphor screen. A reaction that contained no active enzyme was used as a negative control, and a reaction without inhibitor was used as the positive control.

Detection of the effect of compounds on cell based pERK1/2 activity in WM266.4 cells was performed using ELISA kits (Invitrogen) and strictly according to the manufacturer instructions.

4.7. Acute oral toxicity

Five thousand milligrams of compound 27e per kilogram of bodyweight was administered to ten healthy rats by oral gavage. The animals were observed for mortality, signs of gross toxicity and behavioral changes at least once daily for 14 days. Bodyweights were recorded prior to administration and again on Day 7 and 14. All animals survived and appeared active and healthy throughout the study. With the exception of one male that exhibited a loss in body weight between Day 7 and 14, all animals gained bodyweight over the 14-day observation period. There were no signs of gross toxicity or abnormal behavior.

4.8. Docking

The pdb file about the crystal structure of the BRAF kinase domain bound to SB-590885 (3FB8.pdb) was obtained from the RCSB protein data bank (http://www.pdb.org). The molecular docking procedure was performed by using CDOCKER protocol for receptor-ligand interactions section of Discovery Studio 3.1 (Accelrys Software Inc, San Diego, CA). Initially both the ligands and the receptor were pretreated. For ligand preparation, the 3D structures of all the steroidal compounds were generated with ChemBioOffice 2008 and optimized with MMFF94 method. For enzyme preparation, the hydrogen atoms were added with the pH of the protein in the range of 6.5–8.5. CDOCKER is an implementation of a CHARMm based molecular docking tool using a rigid receptor.[25] It includes following steps:

(1) A series of ligand conformations are generated using high temperature molecular dynamics with different random seeds.
(2) Random orientations of the conformations are generated by translating the center of the ligand to a specified position within the receptor active site, and making a series of random rotations. A softened energy is calculated and the orientation is kept when it is less than a specified limit. This process repeats until either the desired number of low-energy orientations is obtained, or the test times of bad orientations reached the maximum number.
(3) Each orientation is subjected to simulated annealing molecular dynamics. The temperature is heated up to a high temperature then cooled to the target temperature. A final energy minimization of the ligand in the rigid receptor using non-softened potential is performed.
(4) For each of the final pose, the CHARMm energy (interaction energy plus ligand strain) and the interaction energy alone are figured out. The poses are sorted according to CHARMm energy and the top scoring (most negative, thus favorable to binding) poses are retained. The whole BRAFkinase domain defined as a receptor and the site sphere was selected based on the ligand binding location of SB-590885, then the SB-590885 removed and the ligands prepared by us was placed during the molecular docking procedure. CHARMm was selected as the force field. The molecular docking was performed with a simulated annealing method. The heating steps were 2000 with 700 of heating target temperature. The cooling steps were 5000 with 300 cooling target temperature. Ten molecular docking poses saved for each ligand were ranked according to their dock score function. The pose with the highest -CDOCKER energy was chosen as the most suitable pose.

4.9. QSAR model

A subset of 35 compounds was utilized as a training set for QSAR modeling. Since it is essential to assess the predictive power of the resulting QSAR models on an external set of inhibitors, the remaining 7 molecules (ca. 20% of the dataset) were employed as an external test subset for validating the QSAR models by the Diverse Molecules protocol in Discovery Studio 3.1. The selected test compounds are: **26a, 28a, 28e, 29b, 30d, 31d, 32b**.

The inhibitory abilities of the compounds in these literatures [IC_{50} (mol/L)] was changed to the minus logarithmic scale [pIC_{50} (mol/L)] and then used for subsequent QSAR analyses as the response variable.

In Discovery Studio, the CHARMm force field is used and the electrostatic potential and the van der Waals potential are treated as separate terms. A +1e point charge is used as the electrostatic potential probe and distance-dependent dielectric constant is used to mimic the solvation effect. For the van der Waals potential a carbon atom with a 1.73 Å radius is used as a probe. The truncation for both the steric and the electrostatic energies was set to 30 kcal/mol. The standard parameters implemented in Discovery Studio 3.1 were used.

A Partial Least-Squares (PLS) model is built using energy grids as descriptors. QSAR models were built using the created 3D-QSAR protocol of Discovery Studio 3.1.

Acknowledgment

This work was financed by NSFC (No. J1103512), by Agriculture Research Project (NY1002), by PCSIRT (IRT1020) and by Natural Science Foundation of Jiangsu Province (BK2009234).

References and notes

1. Wellbrock, C.; Karasarides, M.; Marais, R. *Nat. Rev. Mol. Cell Biol.* **2004**, *5*, 875.
2. Hoshino, R.; Chatani, Y.; Yamori, T.; Tsuruo, T.; Oka, H.; Yoshida, O.; Shimada, Y.; Ari-i, S.; Wada, H.; Fujimoto, J.; Kohno, M. *Oncogene* **1999**, *18*, 813.
3. Davies, H.; Bignell, G. R.; Cox, C.; Stephens, P.; Edkins, S.; Clegg, S.; Teague, J.; Woffendin, H.; Garnett, M. J.; Bottomley, W.; Davis, N.; Dicks, N.; Ewing, R.; Floyd, Y.; Gray, K.; Hall, S.; Hawes, R.; Hughes, J.; Kosmidou, V.; Menzies, A.; Mould, C.; Parker, A.; Stevens, C.; Watt, S.; Hooper, S.; Wilson, R.; Jayatilake, H.; Gusterson, B. A.; Cooper, C.; Shipley, J.; Hargrave, D.; Pritchard-Jones, K.; Maitland, N.; Chenevix-Trench, G.; Riggins, G. J.; Bigner, D. D.; Palmieri, G.; Cossu, A.; Flanagan, A.; Nicholson, A.; Ho, J. W. C.; Leung, S. Y.; Yuen, S. T.; Weber, B. L.; Siegler, H. F.; Darrow, T. L.; Paterson, H.; Marais, R.; Marshall, C. J.; Wooster, R.; Stratton, M. R.; Futreal, P. A. *Nature* **2002**, *417*, 949.
4. Gorden, A.; Osman, I.; Gai, W. M.; He, D.; Huang, W. Q.; Davidson, A.; Houghton, A. N.; Busam, K.; Polsky, D. *Cancer Res.* **2003**, *63*, 3955.
5. Brose, M. S.; Volpe, P.; Feldman, M.; Kumar, M.; Rishi, I.; Gerrero, R.; Einhorn, E.; Herlyn, M.; Minna, J.; Nicholson, A.; Roth, J. A.; Albelda, S. M.; Davies, H.; Cox, C.; Brignell, G.; Stephens, P.; Futreal, P. A.; Wooster, R.; Stratton, M. R.; Weber, B. L. *Cancer Res.* **2002**, *62*, 6997.
6. Kimura, E. T.; Nikiforova, M. N.; Zhu, Z. W.; Knauf, J. A.; Nikiforov, Y. E.; Fagin, J. A. *Cancer Res.* **2003**, *63*, 1454.
7. Xu, X. L.; Quiros, R. M.; Gattuso, P.; Ain, K. B.; Prinz, R. A. *Cancer Res.* **2003**, *63*, 4561.
8. Wan, P. T. C.; Garnett, M. J.; Roe, S. M.; Lee, S.; Niculescu-Duvaz, D.; Good, V. M.; Jones, C. M.; Marshall, C. J.; Springer, C. J.; Barford, D.; Marais, R. *Cell* **2004**, *116*, 855.
9. Gray-Schopfer, V. C.; Dias, S. D.; Marais, R. *Cancer Metastasis Rev.* **2005**, *24*, 165.
10. Sommers, J. A.; Sharma, S.; Doherty, K. M.; Karmakar, P.; Yang, Q.; Kenny, M. K.; Harris, C. C.; Brosh, R. M. *Cancer Res.* **2005**, *65*, 1223.
11. Karasarides, M.; Chiloeches, A.; Hayward, R.; Niculescu-Duvaz, D.; Scanlon, I.; Friedlos, F.; Ogilvie, L.; Hedley, D.; Martin, J.; Marshall, C. J.; Springer, C. J.; Marais, R. *Oncogene* **2004**, *23*, 6292.
12. King, A. J.; Patrick, D. R.; Batorsky, R. S.; Ho, M. L.; Do, H. T.; Zhang, S. Y.; Kumar, R.; Rusnak, D. W.; Takle, A. K.; Wilson, D. M.; Hugger, E.; Wang, L.; Karreth, F.; Lougheed, J. C.; Lee, J.; Chau, D.; Stout, T. J.; May, E. W.; Rominger, C. M.; Schaber, M. D.; Luo, L.; Lakdawala, A. S.; Adams, J. L.; Contractor, R. G.; Smalley, K. S. M.; Herlyn, M.; Morrissey, M. M.; Tuveson, D. A.; Huang, P. S. *Cancer Res.* **2006**, *66*, 11100.
13. Wilhelm, S. M.; Carter, C.; Tang, L. Y.; Wilkie, D.; McNabola, A.; Rong, H.; Chen, C.; Zhang, X. M.; Vincent, P.; McHugh, M.; Cao, Y. C.; Shujath, J.; Gawlak, S.; Eveleigh, D.; Rowley, B.; Liu, L.; Adnane, L.; Lynch, M.; Auclair, D.; Taylor, I.; Gedrich, R.; Voznesensky, A.; Riedl, B.; Post, L. E.; Bollag, G.; Trail, P. A. *Cancer Res.* **2004**, *64*, 7099.
14. Ibrahim, P. N.; Zhang, J.; Cho, H.; Mamo, S.; Bremer, R.; Gillette, S.; Kumar, A.; Fong, D.; Wang, W.; Zhu, Y.-L.; Marimuthu, A.; Suzuki, Y.; Lam, B.; Rice, J.; Tsai, J.; Settachatgul, C.; Shelloe, R.; Cantwell, J.; West, B.; Powell, B.; Habets, G.; Zhang, C.; Artis, D. R.; Hirth, P.; Bollag, G. *Abstr. Paper Am. Chem. Soc.* **2006**, 232.
15. McDermott, U.; Sharma, S. V.; Dowell, L.; Greninger, P.; Montagut, C.; Lamb, J.; Archibald, H.; Raudales, R.; Tam, A.; Lee, D.; Rothenberg, S. M.; Supko, J. G.; Sordella, R.; Ulkus, L. E.; Iafrate, A. J.; Maheswaran, S.; Njauw, C. N.; Tsao, H.; Drew, L.; Hanke, J. H.; Ma, X.-J.; Erlander, M. G.; Gray, N. S.; Haber, D. A.; Settleman, J. *Proc. Natl. Acad. Sci. U.S.A.* **2007**, *104*, 19936.
16. Takle, A. K.; Brown, M. J. B.; Davies, S.; Dean, D. K.; Francis, G.; Gaiba, A.; Hird, A. W.; King, F. D.; Lovell, P. J.; Naylor, A.; Reith, A. D.; Steadman, J. G.; Wilson, D. M. *Bioorg. Med. Chem. Lett.* **2006**, *16*, 378.
17. Ridley, R. G.; Hofheinz, W.; Matile, H.; Jaquet, C.; Dorn, A.; Masciadri, R.; Jolidon, S.; Richter, W. F.; Guenzi, A.; Girometta, M. A.; Urwyler, H.; Huber, W.; Thaithong, S.; Peters, W. *Antimicrob. Agents Chemother.* **1846**, *1996*, 40.
18. De, D. Y. D.; Krogstad, F. M.; Byers, L. D.; Krogstad, D. J. *J. Med. Chem.* **1998**, *41*, 4918.
19. Azarifar, D.; Ghasemnejad, H. *Molecules* **2003**, *8*, 642.
20. Cox, C. D.; Torrent, M.; Breslin, M. J.; Mariano, B. J.; Whitman, D. B.; Coleman, P. J.; Buser, C. A.; Walsh, E. S.; Hamilton, K.; Schaber, M. D.; Lobell, R. B.; Tao, W. K.; South, V. J.; Kohl, N. E.; Yan, Y. W.; Kuo, L. C.; Prueksaritanont, T.; Slaughter, D. E.; Li, C. Z.; Mahan, E.; Lu, B.; Hartman, G. D. *Bioorg. Med. Chem. Lett.* **2006**, *16*, 3175.
21. Havrylyuk, D.; Zimenkovsky, B.; Vasylenko, O.; Zaprutko, L.; Gzella, A.; Lesyk, R. *Eur. J. Med. Chem.* **2009**, *44*, 1396.
22. Blackburn, C.; Duffey, M. O.; Gould, A. E.; Kulkarni, B.; Liu, J. X.; Menon, S.; Nagayoshi, M.; Vos, T. J.; Williams, J. *Bioorg. Med. Chem. Lett.* **2012**, *20*, 4795.
23. Padayatty, S. J.; Riordan, H. D.; Hewitt, S. M.; Katz, A.; Hoffer, L. J.; Levine, M. *Can. Med. Assoc. J.* **2006**, *174*, 937.
24. Kirkpatrick, P. *Nat. Rev. Drug Disc.* **2004**, *3*, 299.
25. Wu, G. S.; Robertson, D. H.; Brooks, C. L.; Vieth, M. *J. Comput. Chem.* **2003**, *24*, 1549.